

THESIS FOR THE DEGREE OF LICENTIATE OF ENGINEERING

# Weld Cracking in Precipitation Hardening Ni-based Superalloys

Fabian Hanning



**CHALMERS**

Department of Industrial and Materials Science  
CHALMERS UNIVERSITY OF TECHNOLOGY  
Gothenburg, Sweden

Weld Cracking in Precipitation Hardening Ni-based Superalloys  
Fabian Hanning

© Fabian Hanning, 2018

Technical report no IMS-2018-7

Department of Industrial and Materials Science  
Chalmers University of Technology  
SE-412 96 Gothenburg  
Sweden  
Telephone + 46 (0)31-772 1000

Printed by Chalmers Reproservice  
Gothenburg, Sweden 2018

# Weld Cracking in Precipitation Hardening Ni-based Superalloys

Fabian Hanning

Department of Industrial and Materials Science  
Chalmers University of Technology

## Abstract

Manufacturing of hot structural components for aero engines requires the materials being used to be weldable. The high demands on strength and temperature resistance make nickel based superalloys the material of choice for this application. Alloy 718 has been the standard grade for several years, providing high strength at elevated temperatures while being weldable due to the relatively slow precipitation kinetics of its hardening phase gamma double prime. Increasing operating temperatures as well as intermittent cycling of land-based gas and steam turbines motivate research on highly temperature stable alloys such as nickel based superalloys. Increased temperature stability of precipitation hardening superalloys is generally achieved via the gamma prime phase, which in contrast to gamma double prime causes a very rapid hardening effect in the material.

Rapid hardening of the gamma prime phase can cause strain age cracking (SAC), a cracking phenomenon occurring during heating towards the post weld heat treatment when stress relaxation mechanism coincide with the precipitation of hardening phases. With the general mechanism of SAC being established, detailed knowledge about the material response is necessary to be able to predict the welding behaviour and to prevent SAC. This is especially relevant with regard to newly developed alloys such as Haynes<sup>®</sup> 282<sup>®</sup>, where limited weldability data is available. This work hence sets focus on investigating the weldability of the relatively new superalloy Haynes<sup>®</sup> 282<sup>®</sup>.

It was found that the welding response of Haynes<sup>®</sup> 282<sup>®</sup> is generally good, with the heat input during welding being identified as main effect on the cracking response under the studied conditions. Solidification cracks were observed in the material, while neither heat affected zone liquation cracks nor SAC could be confirmed. A simulative Gleeble test was developed to provide more data on ductility in the SAC temperature range and its dependence on ongoing precipitation reactions during thermal exposure, correlating the loss in ductility with hardness evolution in the material.

**Keywords:** Nickel based superalloys, welding, weldability, post weld heat treatment, weld cracking, strain age cracking



## Preface

This licentiate thesis is based on the work performed at the Department of Industrial and Materials Science between October 2015 and April 2018. The project has been carried out under the supervision of Assoc. Professor Joel Andersson.

The thesis consists of an introductory part followed by the appended papers:

**Paper I:** A Review of Strain Age Cracking in Nickel Based Superalloys

Fabian Hanning and Joel Andersson

*Proceedings of the 7<sup>th</sup> International Swedish Production Symposium, 2016*

**Paper II:** Weldability of wrought Haynes<sup>®</sup> 282<sup>®</sup> repair welded using manual gas tungsten arc welding

Fabian Hanning and Joel Andersson

*Welding in the World, 62:39-45, 2018*

**Paper III:** The effect of exposure time in the temperature range of 750-950°C on the ductility of wrought Haynes<sup>®</sup> 282<sup>®</sup>

Fabian Hanning, Joachim Steffenburg-Nordenström, Joel Andersson

*Manuscript*

## Contribution to the appended papers

- Paper I: The author conducted the literature review and wrote the paper. Joel Andersson contributed by discussions, paper writing and corrections.
- Paper II: Joel Andersson planned the study. The author planned and executed the microstructural investigations, analysed the results and wrote the paper with discussion input and corrections from the co-author.
- Paper III: The author planned the study and carried out the experimental work involving Gleeble testing and general microstructural analysis. The FE-simulations were carried out by Joachim Steffenburg-Nordenström. The author wrote the paper in cooperation with the co-authors.



## Table of Contents

1. Introduction .....	1
1.1. Aim .....	2
2. Superalloys for aero engine applications.....	3
2.1. The gamma prime phase ( $\gamma'$ ).....	3
2.2. Carbides.....	4
2.3. Other phases .....	4
3. Processing of nickel based superalloys .....	7
4. Welding of superalloys.....	9
4.1. Weld cracking.....	9
5. Experimental methods.....	17
5.1. Material .....	17
5.2. Heat treatments.....	17
5.3. Welding .....	18
5.4. Gleeble testing.....	19
5.5. Sample preparation and investigation techniques .....	19
6. Summary of appended papers .....	21
6.1. Literature review (Paper I) .....	21
6.2. Weld cracking behaviour of Haynes <sup>®</sup> 282 <sup>®</sup> (Paper II) .....	22
6.3. Influence of $\gamma'$ precipitation on the ductility of Haynes <sup>®</sup> 282 <sup>®</sup> (Paper III) .....	24
7. Conclusions .....	27
8. Future work .....	29
9. Acknowledgements .....	31
References .....	33





## 1. Introduction

The hot section of aero engines and gas turbines in general represents a severe environment for the materials being used there. The high temperature combined with the requirement of high strength, resistance to creep, fatigue and hot corrosion narrow down the list of applicable materials. Since their development in the mid-20<sup>th</sup> century, nickel based superalloys have been the materials of choice for this demanding application [1].

While for rotating parts, i.e. turbine blades, the development has been going towards single crystal alloys, for large structural parts as e.g. the engine housings or turbine exhaust casings polycrystalline alloys are used due to production constraints. Traditionally such components have been produced as a single piece casting. However, the more recently followed assembly approach combines the advantages of wrought material (high strength) and cast parts (complex geometry) by producing large components out of small parts that are then joined together by welding [2]. This strategy enables weight savings due to a more tailored structure and also reduces production costs as well as lead time by eliminating the need for large castings.

The fabrication concept of course requires the used materials to be readily weldable. The complex microstructure of nickel based superalloys however often results in challenges when they are to be welded. For several years, the standard material has been Alloy 718 due to its temperature stability up to ~650°C and its good fabricability [3]. With the efficiency of the combustion process increasing with temperature, modern jet engines begin to require new materials that are applicable in the more severe environment.

The use of high alloyed, more temperature stable materials often goes hand in hand with an increased risk of weld cracking. For precipitation hardening superalloys one major concern can be strain age cracking (SAC). This cracking phenomenon occurs while heating to solution heat treatment during the post weld heat treatment (PWHT) and is related to the relaxation of weld residual stresses coinciding with the precipitation of hardening phases in the material. The control of SAC was one of the main drivers for the development of Alloy 718 where the sluggish hardening response of its main hardening phase, gamma double prime, makes it almost immune to SAC. Its limited temperature resistance however has led to the development of new alloy compositions, one of them being Haynes<sup>®</sup> 282<sup>®</sup>. This alloy has a 150°C higher maximum service temperature, but uses the gamma prime phase as hardening precipitate whose more rapid precipitation kinetics may adversely affect cracking resistance. Being a fairly new alloy, not much data is available on its weldability and the mechanisms governing weld cracking in the alloy, requiring more detailed investigations.

## **1.1.Aim**

The aim of this research has been to obtain fundamental knowledge about the formation of weld cracking, including hot cracking but with particular interest in SAC. The goal has been defined on a more detailed level in terms of the following objectives:

- To establish the current state of research involving SAC and identify key mechanisms governing SAC
- To investigate the welding performance of the newly developed nickel based superalloy Haynes<sup>®</sup> 282<sup>®</sup> with particular interest in SAC
- To develop a testing approach suitable for the investigation of the SAC mechanism

## 2. Superalloys for aero engine applications

The severe environment present in the hot sections of aircraft engines require highly stable materials in terms of temperature resistance and strength at high temperatures. At the turbine inlet, the temperature is now exceeding 1500°C [4]. This exceeds the melting point of nickel based superalloys by over 100°C, requiring active cooling and the application of thermal barrier coatings to the exposed material. This becomes even more important for structural components, since the precipitation hardening superalloys applied there usually have to be kept below about 800°C [5].

Generally, nickel based superalloys can be grouped into three categories based on their strengthening mechanism: Solid solution strengthening, precipitation hardening and oxide dispersion strengthening. With the former being used where strength requirements are moderate and high temperature resistance and good corrosion properties are necessary, the precipitation hardening grades are the material of choice for structural applications in aero engines.

Numerous superalloys are commercially available, all of which contain of a complex mixture of alloying elements that influence the mechanical properties by various effect on the microstructure. The elements Co, Cr, Fe, Mo, Ta and W are used for solid solution strengthening based on the not too large deviation in atomic radii and electronic structure compared to the nickel atom. The solubility of these elements is hence quite high [6]. Other alloying elements lead to the formation of secondary phases which can be used for precipitation hardening. Typical hardening precipitates and the alloying elements used to form them are the gamma prime phase  $\gamma'$  ( $\text{Ni}_3\text{Al}$ , Ti) and gamma double prime  $\gamma''$  ( $\text{Ni}_3\text{Nb}$ ). Several elements result in the formation of carbides that are often used to control the grain size in the material (W, Ta, Ti, Mo, Nb, Cr). Some elements do however promote the formation of brittle topologically closed packed (TCP) phases (Nb, Ti, V, Zr, Ta, Al, Si) [7]. The possibility of some alloying elements to form different phases, where some phases are needed to obtain the required properties and others being of detrimental nature, requires fundamental knowledge about the physical metallurgy as well as precise process control.

### 2.1. The gamma prime phase ( $\gamma'$ )

The gamma prime phase  $\gamma'$  is the main hardening phase for precipitation strengthened nickel based superalloys. It has the nominal chemical composition  $\text{Ni}_3\text{Al}$  and a face centred cubic crystal structure. Al can be substituted by Ti and Ta, it is hence often denoted as  $\text{Ni}_3(\text{Al,Ti})$  [8]. Its face centred structure, combined with a low mismatch in lattice parameter, makes it coherent with the nickel matrix and allows for homogeneous precipitation within the matrix. This furthermore leads to fast precipitation kinetics, while particle growth is slow [9]. For small particle diameters and during earlier stages of ageing the particle shape is spherical, as shown exemplarily in Figure 1 for Haynes<sup>®</sup> 282<sup>®</sup>

being exposed to 950°C for 30min. Based on lattice mismatch and particle size the shape can however change to cubic or to plates, reducing the surface energy by matching the structure of the matrix.

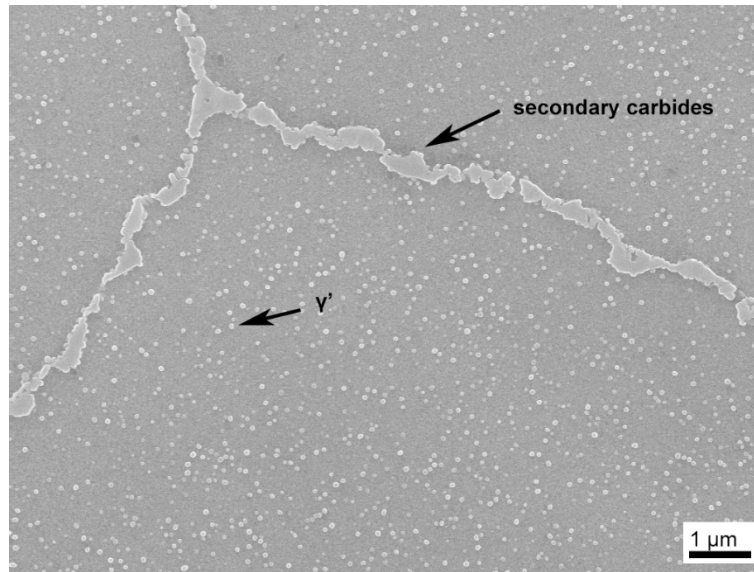
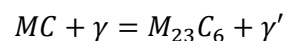


**Figure 1: Microstructure of wrought Haynes® 282®, heat treated at 950°C for 30 min. Gamma prime and secondary carbides at the grain boundaries are indicated by arrows [10] (Paper III).**

## 2.2. Carbides

Different types of carbides can be present in nickel based superalloys. Cubic MC carbides, rich in Ti, Nb or Ta, form at above the solidus temperature of the matrix and are hence present from the primary manufacturing process. The amount and size can change during the subsequent heat treatments, but some MC carbides normally remain in the material. During heat treatments, secondary carbides can form. These are of the  $M_6C$  or  $M_{23}C_6$  type and are usually formed by solid state reactions of the type



Secondary carbides usually form at the grain boundaries and are hence often intentionally precipitated for grain size control as well as to inhibit grain boundary sliding [11]. If present in long, continuous films they however can have detrimental effects on the mechanical properties and weldability.

## 2.3. Other phases

Besides the  $\gamma'$  phase being used as hardening precipitate in most of the precipitation hardening superalloys, weldability issues led to the development of Alloy 718 which instead uses the metastable gamma double prime phase ( $\gamma''$ ). This phase is a body centred tetragonal phase with the nominal chemical composition of  $Ni_3Nb$ . Like the  $\gamma'$  phase it is coherent with the nickel matrix, albeit showing significantly larger mismatch. This results in a steeper increase in strength but also more sluggish precipitation kinetics and reduced thermal stability. Being a metastable phase,  $\gamma''$  decomposes into the

incoherent and stable delta phase ( $\delta$ ), which is accompanied by a loss in strength [11]. The complex chemical composition of superalloys allows for several other phases to be present in the microstructure, notably detrimental TCP phases that can form after long time service exposures [9]. In Nb-bearing alloys such as Alloy 718, the hexagonal laves phase can be present which affects the weldability due to its low melting point [7]. Borides can have the same effect as carbides if finely dispersed, and have been reported to have a positive effect on creep life [12]. Borides can however have a negative effect on heat affected zone (HAZ) liquation cracking, as pointed out further below.



### 3. Processing of nickel based superalloys

Nickel based superalloys are generally available in both wrought and cast form. With the former material form exhibiting a good microstructural homogeneity and high strength, wrought material is not useable for complex shapes without extensive machining, if at all possible. For cast materials on the other hand the shape can be controlled with a much larger degree of freedom. This comes with the disadvantage of a significantly more segregated and inhomogeneous microstructure, resulting in reduced strength. Wrought superalloys are primarily produced using vacuum induction melting (VIM). The obtained ingots are then refined by electro slag re-melting (ESR) and/or vacuum arc re-melting (VAR) techniques [9]. After annealing, drawing and forging, further heat treatments are necessary to obtain the required material properties.

A typical heat treatment procedure is schematically shown in Figure 2. As an initial step, a solution heat treatment is carried out to dissolve secondary phases in the microstructure. Note that such a treatment does not affect primary MC-type carbides since their dissolution temperature lies above the solidus of the matrix. Air cooling or water quenching are used depending on the alloy to prevent microstructural changes during cooling to room temperature. The term ‘mill annealing’ refers to this treatment, representing the material condition typically delivered from the primary manufacturer. Any hardening heat treatments are usually carried out after further manufacturing of components. To achieve the required material properties, age hardening is necessary. This is in most cases done via a two-step process (*cf.* Figure 2). The higher aging temperature is used to obtain the desired amount and morphology of secondary carbides, while during the second aging step the hardening precipitates like  $\gamma'$  are formed in the material. Furthermore, the first step is used to create a supersaturated solid solution during the subsequent aging, which is necessary for efficient aging of  $\gamma'$ . If a bimodal size distribution is desired this step can be further divided into a set of temperatures, as is common practice for Alloy 718 [13]. The same heat treatment procedure also has to be carried out after welding for relieving weld residual stresses and to obtain uniform properties in the whole component. This can cause problems in form of weld cracks as discussed further below.

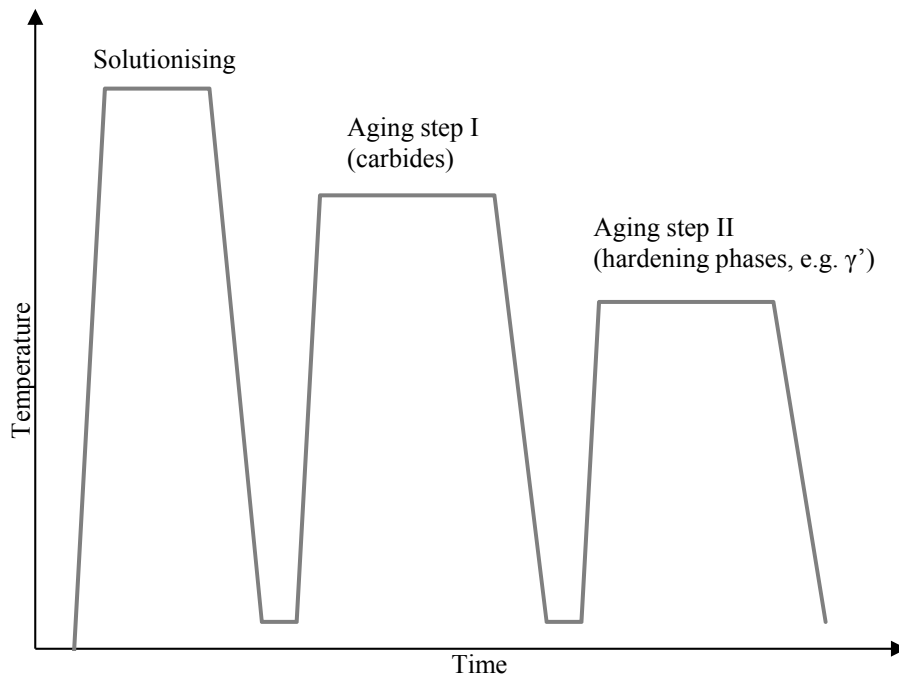


**Figure 2: Schematic heat treatment cycle for nickel based superalloys.**



## **4. Welding of superalloys**

Welding plays a major role in the fabrication of hot structural components using nickel based superalloys. This is based on the possibility to join different materials with small limitations on the shape and previous manufacturing steps. One example is the trend to introduce welding to the fabrication of hot structural parts of jet engines. These components, made out of nickel based superalloys, have traditionally been produced as large single piece castings [2]. By using welding as a joining technique, the combination of high-strength wrought parts and complex shaped cast parts is possible and allows for both weight and cost reductions [14]. Welding processes have experienced significant advancements over the years, which paved their way into the production of structural components in the aero engine industry. The most common techniques used in fabrication are however still gas tungsten arc welding (GTAW), laser beam welding (LBW), plasma arc welding (PAW) and electron beam welding (EBW) [15].

Especially when joining together sophisticated alloys such as superalloys, high demands are placed on process control, but also on the weld geometry. The rapid heating and cooling cycle, together with the mechanical restraint from the joint, can create large amounts of residual stresses in the material [16]. This in turn can lead to cracking and distortion. Furthermore, microstructural changes due to the weld thermal cycle require additional treatments of the welded components. Various PWHT are carried out to relieve weld residual stresses and to obtain the desired microstructural and mechanical properties in the material.

Furthermore, welding of superalloys can result in the formation of weld cracks, with the complex microstructure of superalloys generally making these materials difficult to weld. The knowledge of underlying mechanisms is a requirement to be able to produce crack free welds, explaining the high research interest in weld cracking phenomena in superalloys [15, 17].

### **4.1. Weld cracking**

The cracking mechanisms occurring in nickel based superalloys can be divided into different groups, based on the temperature range within which they occur. Cold cracking is usually not directly connected to welding and includes e.g. hydrogen embrittlement at ambient temperature. Warm cracking phenomena such as strain age cracking and ductility dip cracking occur at high temperatures in the heat affected zone (and fusion zone during multi pass welding operations), but do not require a liquid phase to be present. They are hence also referred to as solid state cracking. Hot cracking occurs at high temperatures and requires the presence of liquid phases, with possible crack formation in both the fusion zone (FZ) and heat affected zone (HAZ) [9].

#### 4.1.1. Solidification cracking

Weld solidification cracking occurs in the FZ, where cracks are formed during the passage of the liquid-solid two-phase region upon cooling. Several theories have been proposed during the last 60 years, but still not all aspects have been fully understood. In general, two main factors can be identified, namely the presence of restraint and a susceptible microstructure. The former can be due to the formation of thermal stresses during cooling, as a temperature and heating/cooling rate gradient between fusion zone and base material is present. The restraint is further influenced by the weld bead geometry, workpiece design and thickness, heat input during welding and mechanical fixture (external restraint). Early theories include the shrinkage-brittleness theory [18] and the strain theory of hot tearing [19]. These have been combined to the generalised theory of super-solidus cracking by Borland in the early 1960s [20]. In general, the solidification process is described as:

- Stage 1: Primary dendrite formation in a continuous liquid with relative movement between all phases being possible.
- Stage 2: Dendrite interlocking, leaving only the liquid as mobile phase.
- Stage 3: Grain boundary development with creation of a semi-continuous network, restricting the liquid phase from moving freely.
- Stage 4: Solidification of the remaining liquid.

It is assumed that cracking occurs exclusively in stage 3, being referred to as 'critical solidification range' (CSR), since backfilling would occur at earlier stages. After complete solidification, contraction stresses are compensated uniformly and no cracking occurs.

In general, a short solidification range is beneficial for the resistance to cracking, as thermal restraint plays an increasing role at lower temperatures. Due to the high alloying content, nickel based superalloys are prone to segregation, resulting in the local suppression of the melting point. Especially minor alloying elements such as P, S, B, C and Zr have a negative influence on the cracking resistance [7, 21], since they are reported to accumulate at grain boundaries and interdendritic areas and form intermetallic compounds such as e.g.  $M_3B_2$  and  $Ni_7Zr_2$  in the case of Inconel 738LC [22, 23]. Alloys containing large amounts of Nb such as Alloy 718 are especially prone to the formation of cracks due to the strong segregation of this element, which causes the formation of NbC carbides and Laves phase eutectics in interdendritic areas. This is accompanied by a significant reduction in melting point in the interdendritic areas [14, 24]. However, the presence of large amounts of eutectic liquid can facilitate backfilling, which reduces the amount of cracks in the material [14, 25, 26].

#### **4.1.2. Heat affected zone liquation cracking**

In contrast to weld solidification cracking, which occurs in the FZ of the weld, HAZ liquation cracking is localised to the partially melted zone, usually referred to as PMZ. This zone lies in the HAZ and is in close proximity to the FZ. Its main characteristic is the presence of a liquid fraction, forming when exceeding the effective solidus temperature during heating. The presence of stresses during subsequent cooling then can cause crack formation. The liquid can form by different mechanisms, namely segregation induced liquation, constitutional liquation and eutectic melting.

Segregation induced liquation is based on the local suppression of the solidus temperature. Especially elements like S, P and B are known to segregate within the microstructure and are usually enriched near grain boundaries. The segregation behaviour of these elements and their effect on the weldability has been thoroughly studied particularly for Alloy 718 [27–37]. Apart from boron, which has been found to have a positive influence on creep resistance and stress rupture life [12], the general effect of these elements is of detrimental nature and their concentrations are usually kept on a minimum level.

Constitutional liquation can occur if second phase particles (i.e. precipitates) are present in the matrix. The mechanism has originally been introduced for maraging steels by Pepe and Savage [38] and later been adapted to explain HAZ liquation cracking in Alloy 718 by Owczarski et al. [39]. A key factor for the mechanism is fast heating, so that particles can survive despite not being thermodynamically stable above the eutectic temperature (assuming the phase interactions can be described by a eutectic system). Under the further assumption of equilibrium conditions at the phase boundary between matrix and particle, a concentration gradient develops around the particle during its subsequent dissolution. When reaching the eutectic temperature, the reaction zone around the particle liquates. It has to be noted that the particle itself does not melt, as e.g. TiC has a melting point far above that of the nickel matrix [7] and only the solute enriched reaction zone contributes to the melt formation. This mechanism has been observed especially for Nb bearing alloys such as Alloy 718 and ALLVAC 718Plus [14, 39] but has also been reported for other precipitation hardening alloys [25, 40–42].

Eutectic melting is only found in cast alloys and related to the strong segregation in interdendritic areas. This has been observed in cast Alloy 718 by various authors [14, 17, 43]. Related to the in general more segregated microstructure of cast alloys they have to be considered more susceptible to HAZ liquation cracking.

#### **4.1.3. Solid state weld cracking phenomena**

In contrast to the hot cracking phenomena described above, solid state cracking does not require a liquid phase to be present in the material; it is hence also referred to as warm cracking. Solid state cracks can occur in several alloy systems and material types.

A material group showing cracks during reheating after welding is the solid solution strengthened nickel based superalloys. The presence of a dip in ductility over an intermediate temperature range was found already in 1912 by Bengough, who investigated aluminium, copper and copper alloys [44]. Rhines and Wray later reported the presence of a ductility dip below the recrystallization temperature in copper alloys, nickel alloys, austenitic stainless steels, titanium alloys and aluminium alloys [45]. The mechanism of ductility dip cracking (DDC) proposed by Rhines and Wray is based on grain boundary shearing at temperatures below the recrystallization temperature [45]. Grain boundary shearing to be the reason for DDC has also been found by Arkoosh and Fiore, who investigated Hastelloy X. They attributed the cause of localised deformation at the grain boundaries to excessive intragranular carbide precipitation [46]. While later investigations from Ramirez and Lippold [47, 48] and Noecker and DuPont [49, 50] also found an influence of carbides, they report them to be beneficial if they precipitate at grain boundaries to inhibit grain boundary sliding. It has been found by Yamaguchi et al. that sulphur segregation leads to grain boundary embrittlement and hence causes DDC [51]. The negative effect of sulphur and other impurities like phosphorous and hydrogen has also been reported in later studies by Collins et al. [52], Nishimoto et al. [53–55] and Saida et al [56]. However, Ramirez and Lippold found that, while impurities have negative impact, the absence of S and P cannot completely prevent ductility dip cracking [47, 48]. They proposed that the main influencing factor is grain boundary tortuosity, leading to a more resistant material due to reduced strain concentration. This is in good agreement with the findings of Noecker and DuPont [49, 50] and has also more recently been confirmed by Chen et al [57].

The phenomenon of reheat cracking has been investigated by various authors for austenitic stainless steels and ferritic low alloy CrMoV steels. It has also been referred to as stress relief cracking in some papers, as this has been identified as a main influencing factor. Younger and Baker investigated reheat cracking in austenitic steels and found a relationship between cracking susceptibility and strain-induced intragranular carbide precipitation ( $\text{TiC}$ ,  $\text{NbC}$ ,  $\text{M}_{23}\text{C}_6$ ) in the temperature range of 550 to 950°C [58]. Other early works include that of Bentley, who found that V carbide precipitation in CrMoV steels leads to embrittlement [59]. He concludes that a large amount of finely dispersed carbides leads to the highest amount of embrittlement (i.e. a low stress relief temperature, favouring nucleation rather than growth reactions to occur). The reason for the fast carbide precipitation in the grain interior during heating has been attributed to a supersaturation of carbide forming elements due to fast cooling after welding [60]. Other researchers found a negative influence of sulphide precipitation [61] and the presence of carbides at grain boundaries [62]. Dhooge and Vinckier have thoroughly reviewed the available literature to reheat cracking in steels and summarise the available mechanisms as follows [63, 64]:

- Intragranular carbide precipitation, leading to relatively weaker grain boundary areas. The precipitation of carbides at grain boundaries has also been reported and is associated with the formation of denuded zones around grain boundaries (i.e. zones with lower alloy content).
- Precipitates at grain boundaries induce void formation or promote boundary decohesion during grain boundary sliding.
- Stress induced segregation of impurities to grain boundaries, leading to embrittlement.

#### 4.1.4. Strain age cracking

The solid state cracking mechanism that can be observed in precipitation hardening nickel based superalloys is SAC, also referred-to as reheat cracking or PWHT cracking. The general mechanism of SAC has been studied in the early 1960s and 70s by various researchers [65–72]. It is generally accepted that the occurrence of cracks during the PWHT cycle is caused by simultaneous presence of stresses in the HAZ and a low ductility in this region. This is explained as follows. During cooling from welding a significant amount of restraint is built up in the HAZ due to thermal stresses and external weld restraint. The former are caused by the temperature gradient present from base metal to weld fusion zone. The residual stresses are relieved during heating to the PWHT, which coincides with the precipitation of hardening phases (*cf.* Figure 3) [67].

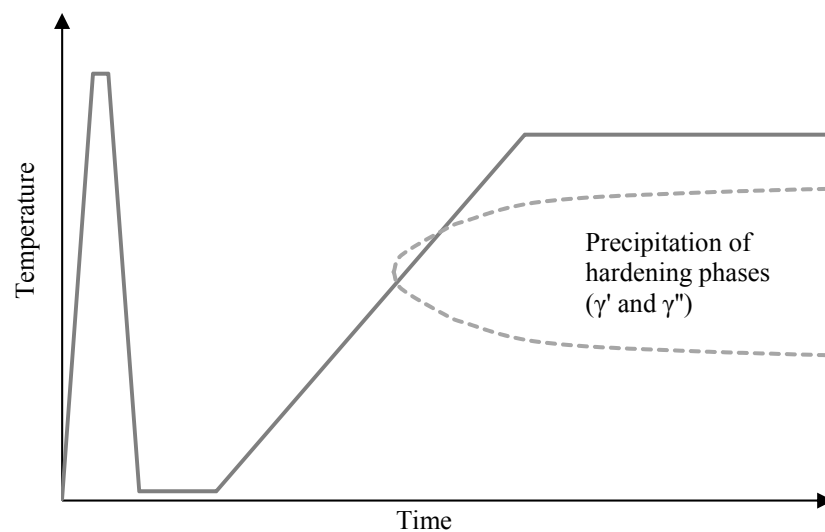


**Figure 3: Schematic time-temperature regime for a welding operation followed by heating to PWHT. The dashed line represents the precipitation curve of a TTT diagram [73] (Paper I).**

The precipitation reaction is believed to lead to a higher strength of the grain interior as compared to the grain boundaries. The deformation (i.e. stress relaxation) is thus localised to the grain boundaries. When grain boundary sliding is not accompanied by volume deformation, high stresses develop especially at grain boundary triple points and intergranular cracks form [45, 58]. Different authors

further claim an additional effect of contraction stresses due to  $\gamma'$  precipitation based on the difference in lattice parameter of the  $\gamma$  matrix and  $\gamma'$  [66, 67, 74, 75].

#### 4.1.4.1. Chemical composition

SAC is a precipitation related phenomenon. It is thus strongly influenced by the chemical composition, which has been investigated by various authors [65, 68, 72, 76]. However, when determining the effect of trace elements the results are often contradicting. This is mainly related to the fact that it is difficult, if not impossible, to alter one elements' concentration without changing that of others at the same time. Combined with the often limited amount of different heats being available for an investigation, the results have to be interpreted with care. The elements forming the hardening phases have the largest influence on the cracking response. An increased Al+Ti content has been reported to lead to higher cracking susceptibility [67, 70]. This is shown in Figure 4, the so-called Prager-Shira diagram [67]. The shown figure has been updated with more recent alloy compositions, where Al+Ti contents above the grey line indicate reduced weldability [73].

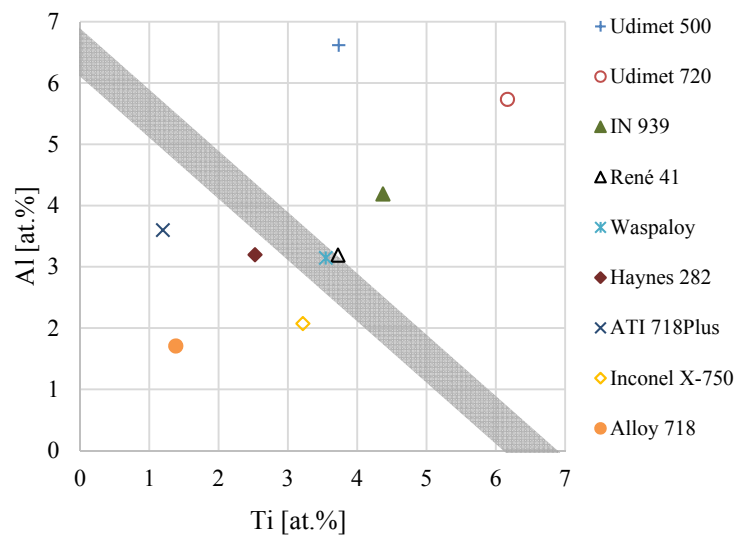


**Figure 4: Al and Ti concentrations of some commercially available superalloys. Low weldability above grey line [73] (Paper I).**

The effect of C has been investigated in several studies and has found to be beneficial due to grain size control [69, 72, 77]. The effect of carbon additions on HAZ liquation cracking should however be considered as well when evaluating the overall weldability of an alloy. Other elements like Fe, Mn and S have been reported to not have a significant effect on SAC, while B can have a similar effect like C and can increase stress rupture life [12, 72]. Research on the role of B has mostly been related to HAZ liquation cracking in Alloy 718, where it was found to have a negative impact [27–37].

#### **4.1.4.2. Effect of microstructure**

Apart from hardening precipitates, the effect of microstructure can be divided into grain size and homogeneity. The former has a positive effect if kept on a low level [76, 78], since the distribution of loads over a larger grain boundary area reduces the local stress level. Inhomogeneities like segregation are more a concern in cast materials, with an effect generally seen in form of increased hot cracking susceptibility. If a welded part is already pre-damaged when put through post weld heat treatment, further cracking can be triggered [17].

The hindering of dislocation movement and hence hardening caused by precipitates like  $\gamma'$  is based on the mismatch with the matrix phase, with a higher mismatch leading to an increased hardening effect. An effect of mismatch on the development of contraction stresses and hence on the SAC susceptibility has been proposed in early studies [66, 67, 74]. More recent computer simulations by Andersson indicate a positive correlation of negative lattice mismatch on the cracking resistance [75]. The lattice parameter change of the  $\gamma$  phase as a function of  $\delta$ ,  $\gamma'$  and  $\gamma''$  has been investigated for Alloy 718 by Liu et al. [79]. They reported a decrease for higher precipitate contents. However, no information is available about the misfit created by the precipitation reactions. Tiley et al. investigated René 88DT by means of synchrotron X-ray and neutron diffraction and reported the lattice mismatch to increase with aging time while initially decreasing as a function of temperature [80]. Another study by Whitmore et al. on Allvac 718Plus showed a small negative lattice mismatch between  $\gamma$  and  $\gamma'$  after aging following on a HAZ simulation with deformation. [81]. Note that the investigation focussed more on morphology and chemical composition. The measurement has been conducted at room temperature and does hence not necessarily reflect the conditions in the PWHT temperature range in terms of lattice parameter misfit. Measurements of the lattice mismatch during creep in a single crystal nickel based superalloy by Dirand et al. led to the conclusion that the misfit is strongly dependent on temperature, stress and previous plastic deformation [82]. Available data indicates a strong relationship between lattice parameter misfit and SAC, quantifiable data obtained in the time-temperature range where SAC occurs has still to be obtained though.

#### **4.1.4.3. Effect of material condition and welding process**

The crack formation during PWHT is related to low ductility in the HAZ, combined with stress relaxation processes. The localisation to the HAZ is related to a lower strength as compared to the base material. It is thus reasonable that softer base material lowers the susceptibility to SAC. This has been confirmed by several investigations [67, 71, 78, 83, 84]. Fully age hardened base material led to most severe cracking in the heat affected zone. Over-aged material on the other hand has been found to have a beneficial influence, as the lower strength of such a microstructure results in stress relaxation in the base material [78]. The thermal stresses generated during the welding operation strongly depend on

the heat input. This becomes clear when comparing the effect of GTAW and EB welding on SAC. However, a low heat input can in turn lead to HAZ liquation cracking [85–87], thus a balance has to be found to achieve the overall best cracking resistance.

The mechanism and the main influencing factors related to SAC can be summarised as follows [73]:

- Strain
  - Weld restraint
  - Precipitation-induced stress
- Stress relaxation
  - Initial magnitude of stress
  - Time-temperature regime
  - Young's modulus
- Precipitation kinetics
  - Chemical composition
  - Strain (higher dislocation density facilitates nucleation)
- Stress localisation at grain boundaries
  - Grain size
  - Grain boundary conditions (*e.g.* precipitates)



## 5. Experimental methods

### 5.1. Material

Haynes<sup>®</sup> 282<sup>®</sup> is a relatively new  $\gamma'$  hardening superalloy [88], developed to provide increased thermal resistance as compared to that of Alloy 718, which due to its hardening phase  $\gamma''$  can withstand temperatures of up to 650°C. The  $\gamma'$  phase used in Haynes<sup>®</sup> 282<sup>®</sup> instead enables a maximum service temperature of 800°C. The general microstructure of Haynes<sup>®</sup> 282<sup>®</sup> is shown in Figure 5. In the as received mill annealed (i.e. solution heat treated) condition the microstructure only shows strings of primary carbides due to the forging and rolling process.



**Figure 5: Microstructure of Haynes<sup>®</sup> 282<sup>®</sup> in mill-annealed condition, with primary MC carbides visible as strings due to the manufacturing history [10] (Paper III).**

In this thesis, Haynes<sup>®</sup> 282<sup>®</sup> has been investigated in form of a forged bar (**Paper II**) and rolled sheet (**Paper III**). The chemical compositions are given in Table 1. Test specimens have been machined from these parts using abrasive waterjet cutting.

**Table 1: Chemical composition of the investigated Haynes<sup>®</sup> 282<sup>®</sup> in wt.-%.**

	Ni	Cr	Co	Mo	Ti	Al	Fe	Mn	Si	C	B
Forged bar (Paper II)	Bal	19.55	10.46	8.70	2.02	1.45	1.17	0.06	0.07	0.063	0.004
Rolled sheet (Paper III)	Bal	19.49	10.36	8.55	2.16	1.52	0.37	0.05	0.05	0.072	0.005

### 5.2. Heat treatments

While the as received condition was investigated, emphasis has been laid on heat treated conditions. In **Paper II**, these were performed in a vacuum furnace with a heating rate of 4-11°C/min and Ar forced

convection cooling, resulting in a cooling rate of  $>50^{\circ}\text{C}/\text{min}$ . The investigated temperatures were chosen to:

- Dissolve  $\gamma'$  in the material at  $1010^{\circ}\text{C}$ , based on the  $\gamma'$  solvus of  $997^{\circ}\text{C}$  [88]. Exposure time was set to 1h
- Remove secondary  $\text{M}_{23}\text{C}_6$  carbides (solvus  $1019^{\circ}\text{C}$ ) without affecting primary and  $\text{M}_6\text{C}$  carbides at  $1120^{\circ}\text{C}$  (0.5h exposure time). This temperature represents the lower limit of the recommended solution annealing window [89]
- Produce a coarse grained microstructure by heat treating the material at  $1150^{\circ}\text{C}$  for 2h.
- Age harden the material at  $788^{\circ}\text{C}$  for 8h

In **Paper III** a test matrix was developed to study the temperature range where SAC occurs, resulting in 5 investigated temperatures ( $750$ - $950^{\circ}\text{C}$ ) and 12 exposure times (5-1800s), as shown in Figure 6.

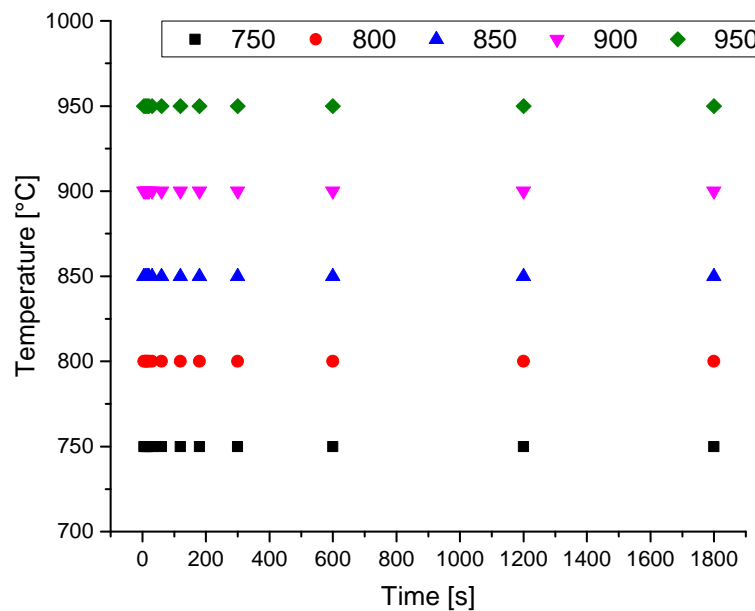


**Figure 6: Temperatures and exposure times used for investigating the SAC susceptibility of Haynes<sup>®</sup> 282<sup>®</sup> [10] (Paper III).**

### 5.3. Welding

Manual GTAW has been used in **Paper II**. Circular grooves were filled with Haynes<sup>®</sup> 282<sup>®</sup> filler wire using a tungsten-2% thorium (WT-20) electrode. Ar gas has been used as shielding gas with a nozzle gas flow of 8-15l/min. A matching chemistry filler material in the form of 1.14mm wire has been used with negative polarity and two welding currents, 120 and 140A. The interpass temperature was approximately  $50^{\circ}\text{C}$  and was reached by quenching with Ar gas in between layer deposition.

## 5.4. Gleeble testing

A Gleeble 3800 thermomechanical simulator has been used in **Paper III** to investigate the influence of exposure time on the SAC susceptibility of Haynes<sup>®</sup> 282<sup>®</sup>. Figure 7 shows the test setup used, while testing parameters are listed in Table 2.

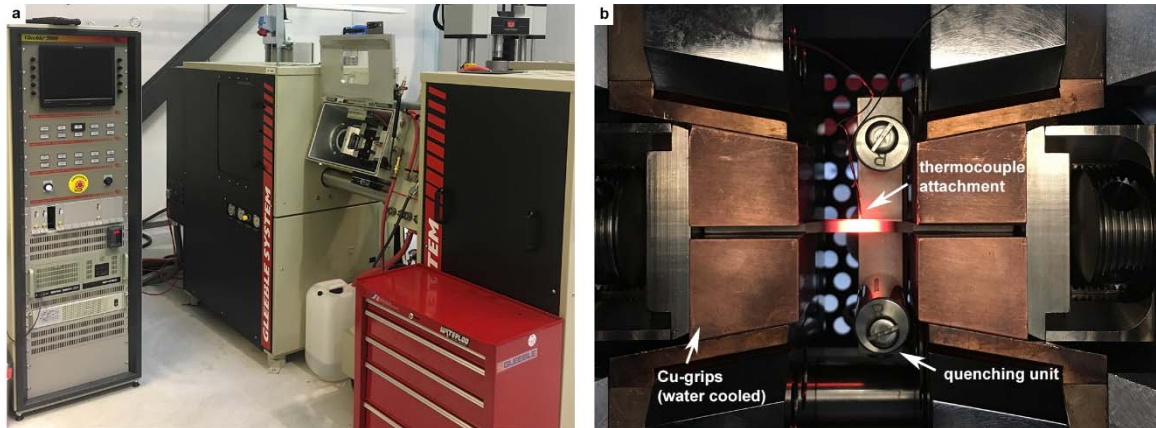


**Figure 7: Gleeble 3800 system (a), test specimen during heating, with thermocouple placement, copper grips and quenching unit indicated by white arrows (b).**

**Table 2: Parameters used for Gleeble testing in Paper III.**

Temperature [°C]	750	800	850	900	950							
Exposure time [s]	5	10	15	20	30	60	120	180	300	600	1200	1800
Heating rate [°C/s]	1000											
Cooling rate (T>500°C) [°C/s]	100											
Stroke rate [mm/s]	55											
Chamber pressure [mbar]	0.1											
Thermocouple	Type K											

## 5.5. Sample preparation and investigation techniques

### 5.5.1. Metallographic preparation

Samples have been mounted in hot mounting resin, followed by automatic grinding and polishing. For microstructural analysis samples were electrolytically etched with 10wt.-% oxalic acid at 3V DC for 3-5s. To analyse  $\gamma'$  in Paper III, a second etchant has been used which removes  $\gamma'$  and carbides while leaving the matrix unaffected. This has been found to lead to more accurate results in image

analysis [90]. The etchant consists of 50ml 37wt.-% HCl, 25ml 65wt.-% HNO<sub>3</sub>, 2g CuCl<sub>2</sub> and 200ml DI H<sub>2</sub>O. Samples were submersed for 40s at room temperature.

### **5.5.2. Microstructural analysis**

Microstructural characterization was initially carried out using light optical microscopy. In the case of crack analysis, non-etched samples were used as a first step. An Olympus BX60M light optical microscope has been used for all investigations. For area measurements an Olympus SZX 9 stereo microscope was used. Selected samples were further investigated using electron microscopy, for which a Leo 1550 FEG SEM, equipped with Oxford instruments EDS and EBSD detectors, and a ZEISS Evo 50 SEM have been used.

### **5.5.3. Hardness testing**

A Shimadzu HMV-2 microhardness tester has been used for measuring Vickers hardness with a force of 0.5 kgf (HV0.5). Measured values represent the average of 5 indentations.

### **5.5.4. JMatPro modelling**

JMatPro 8.0 in conjunction with the nickel based superalloy database was used to model the phase stability of the investigated alloys.

## **6. Summary of appended papers**

### **6.1. Literature review (Paper I)**

Paper I reviewed the literature to identify the underlying mechanisms and influencing factors of SAC. The results of the paper have partially been used in the introduction part of this thesis. The publication of research on SAC over the years has shown that while initial investigations focussed on the general mechanism, more novel research focussed on the development of testing procedures using modern equipment and the investigation of new alloys.

A second part of the paper was the evaluation of test methods available to assess the susceptibility towards SAC. It was found that several methods have been developed over the years, none of them being able to address all aspects of SAC. Especially for new alloys, welding trials can provide a good impression about the actual welding response of the material, which can then be used for further, more controlled studies. Screening tests are important for investigating the relative resistance towards SAC of different alloys.

One of the more commonly used testing approaches follows the idea of simulating the slow heating to PWHT, combined with acquiring ductility data in the temperature range where SAC occurs. This test is referred-to as constant heating rate test (CHRT) [76]. While for the original test a clamshell furnace was used, the use of the Gleeble thermomechanical simulator enables fast heating and cooling cycles that are comparable to those present during welding. This results in the ability to add a fast heating and cooling cycle in advance of the CHRT part to create a microstructure similar to that found in the HAZ of welds where SAC occurs, with the thermal cycle of the test schematically shown in Figure 8. The modified CHRT takes advantage of the more capable testing equipment that is nowadays available in welding research and enables the screening of different alloys based on their susceptibility towards SAC. The testing of microstructures corresponding to those found in the HAZ of actual welds ensures that the test results can be related to results found in real applications. While requiring a metallographic investigation of tested samples, testing HAZ simulated microstructures furthermore includes the effect of potential weaknesses such as liquation cracks that can form during the welding process. The effect of such a pre-damaged microstructure has been found to negatively affect the material performance during simulated PWHT cycles.

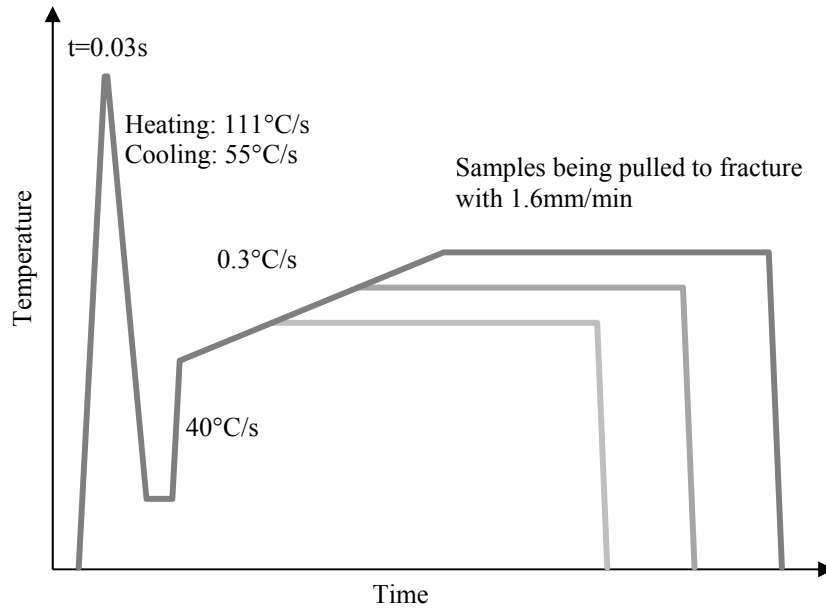


**Figure 8: Time-temperature cycle of the modified CHRT test [73] (Paper I).**

While useful for screening purposes, such a test cannot provide insight into underlying mechanisms, requiring specialized testing methods. Since SAC is a precipitation related cracking phenomenon, the investigation of the precipitation kinetics in the SAC temperature range, combined with short exposure times in the range of PWHT heating rates, could provide a better understanding of this cracking phenomenon.

## **6.2. Weld cracking behaviour of Haynes<sup>®</sup> 282<sup>®</sup> (Paper II)**

Paper II addressed the weld cracking susceptibility of Haynes<sup>®</sup> 282<sup>®</sup> during manual repair GTAW. The study was aimed to provide information about the welding response of Haynes<sup>®</sup> 282<sup>®</sup> under realistic conditions.

Irrespective of welding parameters that have been applied in the study (with 120A welding current being typical welding conditions and 140A representing a more severe environment), no cracks were present in the base metal HAZ. Instead, all cracking was confined to the FZ. No correlation between base metal heat treatment history and cracking response could be observed. Instead, the cracking response was strongly influenced by the heat input, with the use of 140A welding current leading to 1.5x more cracks in the weld deposit layers, as visible in Figure 9.

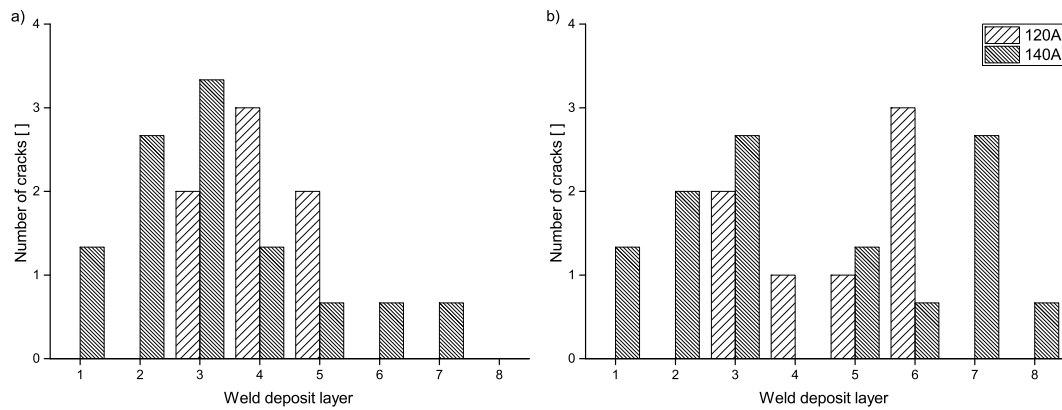


**Figure 9: Total number of cracks per weld deposit layer. a Pre weld heat-treated discs (1-4). b Pre + post weld heat treated discs (5-8). Results for 140A are normalized to account for differences in sampling size for the two conditions [91] (Paper II).**

Furthermore, it can be observed that the cracking response is independent of both pre weld microstructure and PWHTs (cf. total number of cracks in Figure 9 a and b). Further supported by microstructural analysis showing a dendritic structure on the crack surfaces and the location on solidification grain boundaries the cracks were classified as solidification cracks. Small voids without signs of liquid phases being present were also found in the FZ layers. These voids were initially considered to be potential SAC. The EDS analysis however revealed the presence of aluminium-rich oxides. This led to the assumption that the voids are in fact related to oxide layers present from the welding process which have not been properly removed, cf. Figure 10.

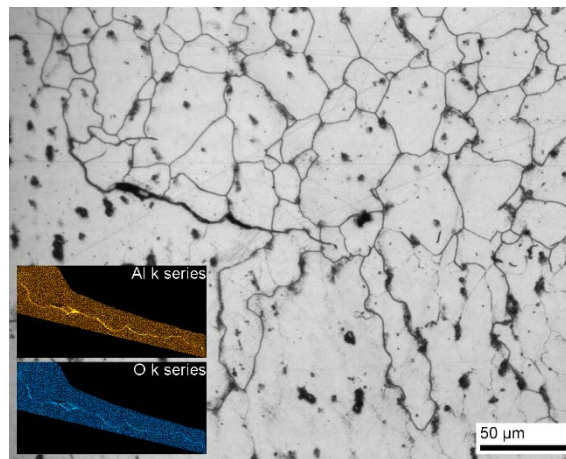


**Figure 10: Aluminium-rich oxide layer at a presumed start location (140A welding current) [91] (Paper II).**

Hardness measurements in both FZ layers and base metal HAZ revealed that 3-4 weld deposit layers are necessary for the hardness to exceed 300 HV in the weld metal. The HAZ showed the same trend, but a slightly quicker hardening response, with only two weld deposit layers being required to reach this hardness level. The absence of SAC in the material suggests that either the weld residual stresses

were below a critical level or that the hardening response was too slow for SAC to occur in the material.

The repair welding study indicates that SAC is not a major concern and instead solidification cracking has to be expected when welding Haynes<sup>®</sup> 282<sup>®</sup>. This is a good sign for the application of the alloy as a replacement for Alloy 718. Nevertheless, the mechanism of SAC and the resistance of candidate alloys for future application in the aero engine sector need to be further investigated. This is especially important with view on the recent trend to introduce additive manufacturing techniques into the production of engine and turbine components. With processes like selective laser melting there is a risk of crack formation during post build processing, with strong similarities to welding related problems such as SAC.

### **6.3. Influence of $\gamma'$ precipitation on the ductility of Haynes<sup>®</sup> 282<sup>®</sup> (Paper III)**

With the modified CHRT being developed for screening purposes, it comes short in providing insight into mechanisms ongoing in the material. To be able to relate the material response found in the CHRT to microstructural changes, a new testing procedure has been developed in **Paper III** [10]. The general observation of the CHRT, the loss of ductility in the intermediate temperature range, has been taken as a starting point for the test design. With the loss in ductility being not as severe for alloys with reduced amount of hardening elements such as Al and Ti, the susceptibility to SAC strongly depends on alloy composition [17, 92, 93]. Following from that an interrelationship of ductility and precipitation kinetics has been proposed [67], but no quantified data is available yet.

Since the CHRT uses a constant heating rate to the different test temperatures, the effect of hardening reactions cannot be investigated. The new approach hence utilises fast heating of 1000°C/s and subsequent isothermal exposure to obtain microstructures with varying precipitation structure. The test temperatures have been selected based on the results of a previous CHRT investigation such that the test covers the temperature range around the drop in ductility [17]. In the CHRT, the total exposure time in the precipitation temperature range is 20-30min, considering both the heating and mechanical testing parts of the test [92, 93]. Hence, the two longest exposure times were considered to reflect comparable conditions to those of the CHRT. The test results show a clear influence of exposure time on the ductility, as indicated in Figure 11.



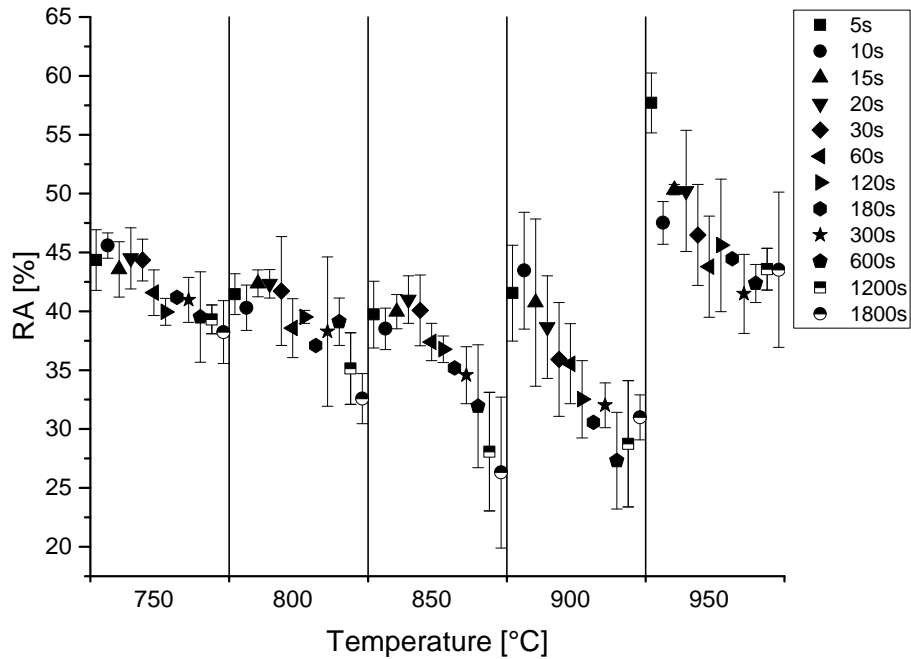


**Figure 11: Reduction in area as a function of temperature and time. Average of three measurements with respective 95% confidence interval (Paper III).**

This loss in ductility could be attributed to the difference in precipitation structure in the material, as hardness values correlate well with the observed ductility, as shown in Figure 12. Together with microstructural and fractographic analysis the reason for the drop in ductility could be related to the following factors:

The ductility drop is strongly coupled to the onset of hardening reactions in the material. At 750°C the only moderate reduction in ductility has been related to the slower precipitation kinetics at this temperature. For higher temperatures nucleation and growth of  $\gamma'$  occurs more rapidly, which was confirmed by particle analysis. The heat treatments also led to the precipitation of secondary carbides on grain boundaries. An effect on the fracture behaviour at 950°C could however not be detected, i.e. the fracture mode remained ductile transgranular, albeit with a reduction in ductility for longer exposure times.

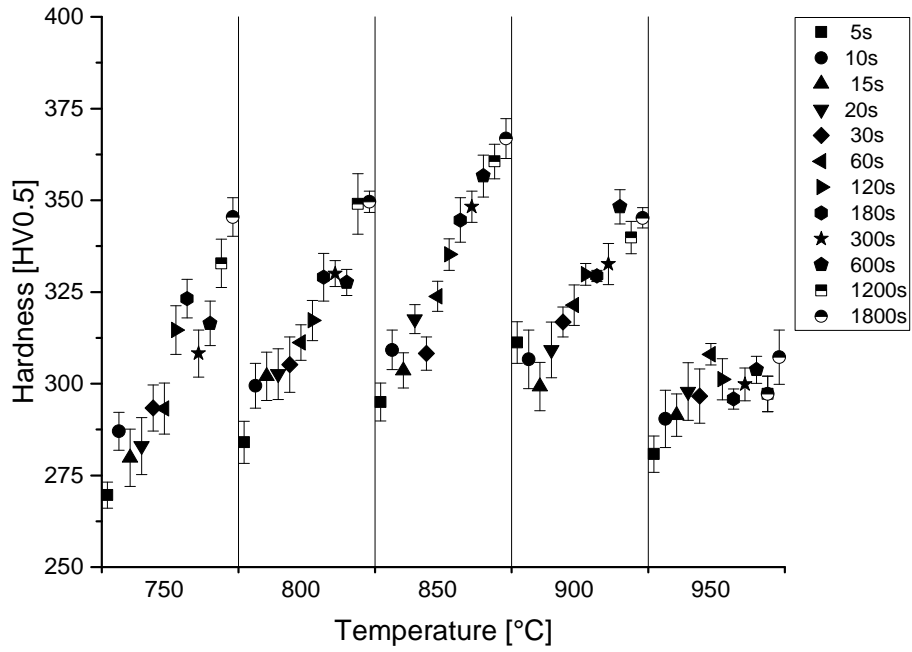


**Figure 12: Hardness evolution in the SAC temperature range (Paper III).**

The results provide new data to better understand the underlying mechanism of SAC. When used as a screening test for different alloys this test furthermore has the potential to be used to develop threshold criteria for PWHT procedures in terms of heating rate and hence exposure time in the critical temperature range.

## 7. Conclusions

- The literature has been reviewed with focus on SAC and related testing methods. Based on this the following conclusions can be drawn.
  - With the general mechanism being accepted in literature, there is still little data available that links material response (i.e. low ductility) and quantified information about the precipitation kinetics causing it.
  - Out of the numerous testing procedures that have been developed, the CHRT seems to be most promising as a screening test. In light of more modern testing equipment some modifications could improve its results.
- Multi pass manual repair welding showed that wrought Haynes<sup>®</sup> 282<sup>®</sup> exhibits good resistance towards HAZ liquation cracking, while solidification cracking can be a concern depending on process parameters such as heat input.
- The interrelationship of precipitation kinetics and the susceptibility towards SAC can be investigated with a newly developed Gleeble-based testing procedure.
  - Using this procedure, the drop in ductility responsible for the occurrence of SAC has been correlated to the hardening response and precipitation characteristics of Haynes<sup>®</sup> 282<sup>®</sup>.



## 8. Future work

Additional TEM investigations of samples tested in **Paper III** are planned and to be carried out to supplement the results already obtained from SEM analysis. The test method developed in Paper III will be extended to other alloys such as ATI 718Plus<sup>®</sup> or Waspaloy in order to provide an in depth comparison of different materials.

The welding behaviour of cast ATI 718Plus<sup>®</sup> is to be investigated and complemented with temperature measurements in the base metal HAZ. This should provide data for further microstructural studies using the Gleeble system.

The influence of light elements such as B and C on weld cracking in Haynes<sup>®</sup> 282<sup>®</sup> and ATI 718Plus<sup>®</sup> is planned to be investigated using e.g. TEM, Auger and SIMS. This could be carried out on the already available material, and is planned to be set within the framework of a research visit.



## **9. Acknowledgements**

I am deeply grateful to my supervisor Assoc. Professor Joel Andersson and my examiner Professor Lars Nyborg. Thank you for making this research possible and for all the discussions, support and encouragement.

Most of my working time I spend at the welding group at University West in Trollhättan. I would like to say thank you to everyone at the Production Technology Centre at University West for the warm welcome and for making this a great experience. Special thanks go to my fellow PhD students in the welding group for all the discussions and the good time! I am looking forward to continue working together with you.

I thank all my colleagues in the department of Industrial and Materials Science for a friendly work environment and the support I always receive when I am there for a visit.

Finally I want to thank my family. I would not be here today without all your support and encouragement!





## References

1. Decker RF (2006) The evolution of wrought age-hardenable superalloys. *JOM* 58:32–36 . doi: 10.1007/s11837-006-0079-8
2. Sjöberg G (2010) Casting Superalloys For Structural Applications. In: 7th International Symposium on Superalloy 718 and Derivatives. The Minerals, Metals & Materials Society, pp 117–130
3. Schafrik RE, Ward DD, Groh JR (2001) Application of alloy 718 in GE aircraft engines: past, present and next five years. In: Superalloys 718, 625, 706 and Various derivatives. The Minerals, Metals & Materials Society, pp 1–11
4. Lefebvre AH, Ballal DR (2010) Gas Turbine Combustion: Alternative Fuels and Emissions. Taylor & Francis, Boca Raton
5. Donachie MJ, Donachie SJ (2002) Superalloys A Technical Guide. ASM International, Materials Park, OH
6. Stoloff NS (1990) Wrought and P/M Superalloys. In: Metals Handbook. ASM International, Materials Park, OH, pp 950–980
7. DuPont JN, Lippold JC, Kiser SD (2009) Welding metallurgy and weldability of nickel-base alloys. Wiley, Hoboken, N.J.
8. Bürgel R, Maier HJ, Niendorf T (2011) Handbuch Hochtemperatur-Werkstofftechnik Grundlagen, Werkstoffbeanspruchungen, Hochtemperaturlegierungen und -beschichtungen. Springer Fachmedien Wiesbaden, Wiesbaden
9. Sims CT, Stoloff NS, Hagel WC (1987) Superalloys II. Wiley, New York
10. Hanning F, Steffenburg-Nordenström J, Andersson J (2018) The effect of exposure time on the ductility of wrought Haynes® 282® in the temperature range of 750-950°C. Manuscript
11. Reed RC (2006) The Superalloys Fundamentals and Applications. Cambridge University Press, Cambridge, UK; New York
12. Cao W-D, Kennedy RL (1997) Effect and Mechanism of Phosphorous and Boron on Creep Deformation of Alloy 718. In: Superalloys 718, 625, 706 and Various Derivatives. pp 511–520
13. Allegheny Technologies Incorporated (ATI) (2013) ATI 718Plus Alloy Product Brochure
14. Andersson J (2011) Weldability of precipitation hardening superalloys: Influence of microstructure. Doctoral Thesis, Chalmers University of Technology
15. Andersson J (2018) Review of weldability of precipitation hardening Ni- and Fe-Ni-based superalloys. In: Proceedings of the 2018 Superalloy 718 & Derivatives: Energy, Aerospace, and Industrial Applications. The Minerals, Metals & Materials Society, Pittsburgh, USA, p submitted manuscript
16. Peacock HB, Lundin CD, Spruiell JE (1972) Comparison and Analysis of Residual Stress Measuring Techniques and the Effect of Post-Weld Heat Treatment on Residual Stresses in Inconel 600, Inconel X-750 and René 41 Weldments. *WRC Bull* 177:1–24
17. Hanning F (2015) Strain Age Cracking of Nickel Based Superalloys. Master Thesis, Chalmers University of Technology
18. Pumphrey WI, Jennings PH (1948) A Consideration of the Nature of Brittleness at Temperatures Above the Solidus in Castings and Welds in Aluminium Alloys. *J Inst Met* 75:235–256
19. Pellini WS (1952) Strain Theory of Hot Tearing. *Foundry* 80:125-133;192-199

20. Borland JC (1960) Generalized Theory of Super-Solidus Cracking in Welds (and Castings). *Br Weld J* 7:508–512
21. Lippold JC (1983) An Investigation of Heat Affected Zone Cracking in Alloy 800. *Weld J* 62:1s–11s
22. Ojo OA, Richards NL, Chaturvedi MC (2004) Microstructural study of weld fusion zone of TIG welded IN 738LC nickel-based superalloy. *Scr Mater* 51:683–688 . doi: 10.1016/j.scriptamat.2004.06.013
23. Ojo OA, Richards NL, Chaturvedi MC (2006) Study of the fusion zone and heat-affected zone microstructures in tungsten inert gas-welded INCONEL 738LC superalloy. *Metall Mater Trans A* 37:421–433
24. DuPont JN, Robino CV, Marder AR (1998) Solidification and Weldability of Nb-Bearing Superalloys. *Weld J* 77:417s–431s
25. Vishwakarma K (2008) Microstructural Analysis of Weld Cracking in 718 Plus Superalloy. University of Manitoba
26. Lippold JC, Sowards J, Alexandrov J, et al (2008) Weld Solidification Cracking in Solid Solution Strengthened Ni-Base Filler Metals. In: Böllinghaus T, Herold H, Cross CE, Lippold JC (eds) *Hot Cracking Phenomena in Welds II*. Springer Berlin Heidelberg, pp 147–170
27. Andersson J (2005) Allvac 718+, Mikrostruktur vid Värmebehandling och Svetsning. Bachelor Thesis, Bergskolan - The Swedish School of Mining and Metallurgy
28. Kelly TJ (1989) Elemental effects on cast 718 weldability. *Weld J* 68:44s–51s
29. Chaturvedi MC, Chen W, Saranchuk A (1997) The Effect of B Segregation on Heat-Affected Zone Microfissuring in EB Welded Inconel 718. In: *Superalloys 718, 625, 706 and Various Derivatives*. The Minerals, Metals & Materials Society, pp 743–751
30. Vishwakarma KR, Chaturvedi MC (2009) Effect of boron and phosphorus on HAZ microfissuring of Allvac 718 Plus superalloy. *Mater Sci Technol* 25:351–360 . doi: 10.1179/174328407X243032
31. Vincent R (1985) Precipitation around welds in the nickel-base superalloy, Inconel 718. *Acta Metall* 33:1205–1216
32. Thompson RG, Dobbs JR, Mayo DE (1986) The Effect of Heat Treatment on Microfissuring in Alloy 718. *Weld J* 65:299s–304s
33. Huang X, Chaturvedi MC, Richards NL, Jackman J (1997) The effect of grain boundary segregation of boron in cast alloy 718 on HAZ microfissuring—A SIMS analysis. *Acta Mater* 45:3095–3107 . doi: 10.1016/S1359-6454(97)00017-7
34. Ping DH, Gu YF, Cui CY, Harada H (2007) Grain boundary segregation in a Ni–Fe-based (Alloy 718) superalloy. *Mater Sci Eng A* 456:99–102 . doi: 10.1016/j.msea.2007.01.090
35. Chen W, Chaturvedi MC, Richards NL (2001) Effect of boron segregation at grain boundaries on heat-affected zone cracking in wrought INCONEL 718. *Metall Mater Trans A* 32:931–939
36. Benhadad S, Richards NL, Chaturvedi MC (2002) The influence of minor elements on the weldability of an INCONEL 718-type superalloy. *Metall Mater Trans A* 33:2005–2017
37. Alam T, Felfer PJ, Chaturvedi M, et al (2012) Segregation of B, P, and C in the Ni-Based Superalloy, Inconel 718. *Metall Mater Trans A* 43:2183–2191 . doi: 10.1007/s11661-012-1085-9
38. Pepe JJ, Savage WF (1967) Effects of Constitutional Liquation in 18-Ni Maraging Steel Weldments. *Weld J* 46:411s–422s

39. Owczarski WA, Duvall DS, Sullivan CP (1966) A Model for Heat-Affected Zone Cracking in Nickel-Base Superalloys. *Weld J* 45:145s–155s
40. Radhakrishnan B, Thompson RG (1993) The effect of weld Heat-Affected zone (HAZ) liquation kinetics on the hot cracking susceptibility of alloy 718. *Metall Trans A* 24:1409–1422
41. Ojo OA, Richards NL, Chaturvedi MC (2004) Contribution of constitutional liquation of gamma prime precipitate to weld HAZ cracking of cast Inconel 738 superalloy. *Scr Mater* 50:641–646 . doi: 10.1016/j.scriptamat.2003.11.025
42. Ojo OA, Richards NL, Chaturvedi MC (2004) Liquid film migration of constitutionally liquated  $\gamma'$  in weld heat affected zone (HAZ) of Inconel 738LC superalloy. *Scr Mater* 51:141–146 . doi: 10.1016/j.scriptamat.2004.03.040
43. Baeslack WA, Nelson DE (1986) Morphology of weld heat-affected zone liquation in cast alloy 718. *Metallography* 19:371–379
44. Bengough GD (1912) A study of the properties of alloys at high temperatures. *J Inst Met* 7:123–174
45. Rhines FN, Wray PJ (1961) Investigation of the Intermediate Temperature Ductility Minimum of Metals. *ASM Trans Q* 54:
46. Arkoosh MA, Fiore NF (1972) Elevated temperature ductility minimum in Hastelloy alloy X. *Metall Trans* 3:2235–2240 . doi: 10.1007/BF02643237
47. Ramirez A., Lippold J. (2004) High temperature behavior of Ni-base weld metal Part II – Insight into the mechanism for ductility dip cracking. *Mater Sci Eng A* 380:245–258 . doi: 10.1016/j.msea.2004.03.075
48. Ramirez AJ, Lippold JC (2005) New Insight into the Mechanism of Ductility Dip Cracking in Ni-base Weld Metals. In: Böllinghaus T, Herold H (eds) *Hot Cracking Phenomena in Welds*. Springer, Berlin, Heidelberg, pp 19–41
49. Noecker F, DuPont JN (2009) Metallurgical investigation into ductility dip cracking in Ni-based alloys: Part I. *Weld J* 88:7s–20s
50. Noecker FF, DuPont JN (2009) Metallurgical investigation into ductility dip cracking in Ni-based alloys: Part II. *Weld J* 88:62s–77s
51. Yamaguchi S, Kobayashi H, Matsumiya T, Hayami S (1979) Effect of minor elements on hot workability of nickel-base superalloys. *Met Technol* 6:170–175
52. Collins MG, Lippold JC (2003) An investigation of ductility dip cracking in nickel-based filler materials-Part I. *Weld J* 82:288s–295s
53. Nishimoto K, Saida K, Okauchi H (2006) Microcracking in multipass weld metal of alloy 690 Part 1 – Microcracking susceptibility in reheated weld metal. *Sci Technol Weld Join* 11:455–461 . doi: 10.1179/174329306X94291
54. Nishimoto K, Saida K, Okauchi H, Ohta K (2006) Microcracking in multipass weld metal of alloy 690 Part 2 – Microcracking mechanism in reheated weld metal. *Sci Technol Weld Join* 11:462–470 . doi: 10.1179/174329306X94309
55. Nishimoto K, Saida K, Okauchi H, Ohta K (2006) Microcracking in multipass weld metal of alloy 690 Part 3 – Prevention of microcracking in reheated weld metal by addition of La to filler metal. *Sci Technol Weld Join* 11:471–479 . doi: 10.1179/174329306X94318
56. Saida K, Nomoto Y, Okauchi H, et al (2012) Influences of phosphorus and sulphur on ductility dip cracking susceptibility in multipass weld metal of alloy 690. *Sci Technol Weld Join* 17:1–8 . doi: 10.1179/1362171810Y.0000000004

57. Chen JQ, Lu H, Cui W, et al (2014) Effect of grain boundary behaviour on ductility dip cracking mechanism. *Mater Sci Technol* 30:1189–1196 . doi: 10.1179/1743284713Y.0000000431
58. Younger RN, Baker RG (1961) Heat-Affected Zone Cracking in Welded Austenitic Steels During Heat Treatment. *Br Weld J* 8:579–587
59. Bentley KP (1964) Precipitation During Stress Relief of Welds in Cr-Mo-V Steels. *Br Weld J* 11:507–515
60. Swift RA (1971) The Mechanism of Stress Relief Cracking in 2-1/4cr-1mo Steel. *Weld J* 50:195s–200s
61. Shin J, McMahon CJ (1984) Mechanisms of stress relief cracking in a ferritic steel. *Acta Metall* 32:1535–1552 . doi: 10.1016/0001-6160(84)90100-7
62. Meitzner CF, Pense AW (1969) Stress-Relief Cracking in Low-Alloy Steel Weldments. *Weld J* 48:431s–440s
63. Dhooge A, Vinckier A (1987) Reheat cracking—A review of recent studies. *Int J Press Vessels Pip* 27:239–269 . doi: 10.1016/0308-0161(87)90012-3
64. Dhooge A, Vinckier A (1992) Reheat Cracking - A Review of Recent Studies. *Weld World* 30:44–71
65. Hughes WP, Berry TF (1967) A Study of the Strain-Age Cracking Characteristics in Welded René 41 - Phase I. *Weld J* 46:361s–370s
66. Wu KC, Herfert RE (1967) Microstructural Studies of René 41 Simulated Weld Heat-Affected Zones. *Weld J* 46:32s–38s
67. Prager M, Shira CS (1968) Welding of Precipitation-Hardening Nickel-Base Alloys. *WRC Bull* 128:1–55
68. Duvall DS, Owczarski WA (1969) Studies of Postweld Heat-Treatment Cracking in Nickel-Base Alloys. *Weld J* 48:10s–22s
69. Dix AW, Savage WF (1971) Factors influencing strain-age cracking in Inconel X-750. *Weld J* 50:247s–252s
70. McKeown D (1971) Re-Heat Cracking in High Nickel Alloy Heat-Affected Zones. *Weld J* 50:201s–206s
71. Franklin JE, Savage WF (1974) Stress Relaxation and Strain-Age Cracking in Rene 41 Weldments. *Weld J* 53:380s–387s
72. Thamburaj R, Goldak JA, Wallace W (1979) The Influence of Chemical Composition in Post-Weld Heat Treatment Cracking in René 41. *SAMPE Q* 4:6–12
73. Hanning F, Andersson J (2016) A Review of Strain Age Cracking in Nickel Based Superalloys. In: Conference Proceedings of the 7th International Swedish Production Symposium. Lund, SE
74. Schwenk W, Trabold AF (1963) Weldability of René 41. *Weld J* 42:460s–645s
75. Andersson J (2014) Weldability of Ni-Based Superalloys. In: Proceedings of the 8th International Symposium on Superalloy 718 and Derivatives. The Minerals, Metals & Materials Society, pp 249–262
76. Carlton JB, Prager M (1970) Variables Influencing the Strain-Age Cracking and Mechanical Properties of René 41 and Related Alloys. *WRC Bull* 150:13–23
77. Prager M, Sines G (1970) A Mechanism for Cracking During Postwelding Heat Treatment of Nickel-Base Alloys. *WRC Bull* 150:24–32

78. Berry TF, Hughes WP (1969) A Study of the Strain-Age Cracking Characteristics in Welded René 41 - Phase II. *Weld J* 48:505s–513s
79. Liu WC, Xiao FR, Yao M, et al (1997) Relationship between the lattice constant of  $\gamma$  phase and the content of  $\delta$  phase,  $\gamma''$  and  $\gamma'$  phases in inconel 718. *Scr Mater* 37:59–64 . doi: 10.1016/S1359-6462(97)00064-X
80. Tiley J, Srinivasan R, Banerjee R, et al (2009) Application of X-ray and neutron diffraction to determine lattice parameters and precipitate volume fractions in low misfit nickel base superalloys. *Mater Sci Technol* 25:1369–1374 . doi: 10.1179/174328409X399010
81. Whitmore L, Ahmadi MR, Stockinger M, et al (2014) Microstructural investigation of thermally aged nickel-based superalloy 718Plus. *Mater Sci Eng A* 594:253–259 . doi: 10.1016/j.msea.2013.11.037
82. Dirand L, Cormier J, Jacques A, et al (2013) Measurement of the effective  $\gamma/\gamma'$  lattice mismatch during high temperature creep of Ni-based single crystal superalloy. *Mater Charact* 77:32–46 . doi: 10.1016/j.matchar.2012.12.003
83. Thompson EG, Nunez S, Prager M (1968) Practical Solutions to Strain-Age Cracking of René 41. *Weld J* 47:299s–313s
84. Duvall DS, Owczarski WA (1971) Heat Treatments for Improving the Weldability and Formability of Udimet 700. *Weld J* 50:401s–409s
85. Idowu OA, Ojo OA, Chaturvedi MC (2007) Effect of heat input on heat affected zone cracking in laser welded ATI Allvac 718Plus superalloy. *Mater Sci Eng A* 454–455:389–397 . doi: 10.1016/j.msea.2006.11.054
86. Gordine J (1971) Some Problems in Welding Inconel 718. *Weld J* 50:480s–484s
87. Richards NL, Nakkalil R, Chaturvedi MC (1994) The influence of electron-beam welding parameters on heat-affected-zone microfissuring in INCOLOY 903. *Metall Mater Trans A* 25:1733–1745
88. Pike LM (2006) HAYNES® 282™ Alloy - A New Wrought Superalloy Designed for Improved Creep Strength and Fabricability. In: *Proceedings of ASME Turbo Expo 2006: Power for Land, Sea and Air*. ASME, Barcelona, Spain, pp 1031–1039
89. Haynes International Inc. (2008) Haynes 282 Product Brochure
90. Salehi R, Samadi A, Savadkoobi MK (2012) Influence of Etchants on Quantitative/Qualitative Evaluations of the  $\gamma'$  Precipitates in a Nickel-Base Superalloy. *Metallogr Microstruct Anal* 1:290–296 . doi: 10.1007/s13632-012-0043-7
91. Hanning F, Andersson J (2018) Weldability of wrought Haynes® 282® repair welded using manual gas tungsten arc welding. *Weld World* 62:39–45 . doi: 10.1007/s40194-017-0508-z
92. Fawley RW, Prager M (1970) Evaluating the Resistance of René 41 to Strain-Age Cracking. *WRC Bull* 150:1–12
93. Metzler DA (2008) A Gleeble®-based method for ranking the strain-age cracking susceptibility of Ni-based superalloys. *Weld J* 87:249s–256s